forests

MDPI

Article

Spatiotemporal Changes in Vegetation Cover and Soil Moisture in the Lower Reaches of the Heihe River Under Climate Change

Lei Mao [1], Xiaolong Pei [2,*], Chunhui He [3], Peng Bian [1], Dongyang Song [2], Mengyang Fang [4,5], Wenyin Wu [6,7,8,9,10,11], Huasi Zhan [4,5,*], Wenhui Zhou [1] and Guanghao Tian [2]

1 Hohhot General Survey of Natural Resources Center, China Geological Survey, Hohhot 010000, China; maolei@mail.cgs.gov.cn (L.M.); bianpeng@mail.cgs.gov.cn (P.B.); zhouwenhui@mail.cgs.gov.cn (W.Z.)
2 Langfang Comprehensive Survey Center of Natural Resources, China Geological Survey, Langfang 065000, China; songdongyang@mail.cgs.gov.cn (D.S.); tianguanghao@mail.cgs.gov.cn (G.T.)
3 School of Electronic Engineering and Intelligent Manufacturing, Anqing Normal University, Anqing 246133, China; 15155098904@163.com
4 Haikou Marine Geological Survey Center, China Geological Survey, Haikou 571127, China; fangmengyang@mail.cgs.gov.cn
5 Sanya Land-Sea Interface Critical Zone Field Scientific Observation and Research Station, Sanya 572022, China
6 School of Life Science, Anqing Normal University, Anqing 246133, China; 122407@aqnu.edu.cn
7 Huangshan Observation and Research Station for Land-Water Resources, Huangshan 245000, China
8 Changsha Comprehensive Survey Center of Natural Resources, China Geological Survey, Changsha 410600, China
9 Key Laboratory of Tropical Island Land Surface Processes and Environmental Changes of Hainan Province, Haikou 571158, China
10 Key Lab. of Biodiversity Conservation and Characteristic Resource Utilization in Southwest Anhui, Anqing 246133, China
11 Anqing Forestry Technology Innovation Research Institute, Anqing 246001, China
* Correspondence: peixiaolong@mail.cgs.gov.cn (X.P.); zhanhuasi@mail.cgs.gov.cn (H.Z.); Tel.: +86-13222484985 (X.P.)

Abstract: As global climate change intensifies, arid land ecosystems face increasing challenges. Vegetation, a key indicator of climate variation, is highly responsive to meteorological factors such as temperature (Tem), precipitation (Pre), and soil moisture (SM). Understanding how fractional vegetation cover (FVC) responds to climate change in arid regions is critical for mitigating its impacts. This study utilizes MOD13Q1-NDVI data from 2000 to 2022, alongside corresponding Tem, Pre, and SM data, to explore the dynamics and underlying mechanisms of SM and FVC in the context of climate change. The results reveal that both climate change and human activities exacerbate vegetation degradation, underscoring its vulnerability. A strong correlation between FVC and both Tem and Pre suggests that these factors significantly influence FVC variability. In conclusion, FVC in the lower reaches of the Heihe River is shaped by a complex interplay of Tem, Pre, SM, and human activities. The findings provide a scientific basis and decision-making support for ecological conservation and water resource management in the lower reaches of the Heihe River, aiding in the development of more effective strategies to address future climate challenges.

Keywords: arid zone; climate change; response characteristics; soil moisture; vegetation cover

check for updates

Citation: Mao, L.; Pei, X.; He, C.; Bian, P.; Song, D.; Fang, M.; Wu, W.; Zhan, H.; Zhou, W.; Tian, G. Spatiotemporal Changes in Vegetation Cover and Soil Moisture in the Lower Reaches of the Heihe River Under Climate Change. *Forests* **2024**, *15*, 1921. https://doi.org/10.3390/f15111921

Academic Editor: David Ellison

Received: 19 September 2024
Revised: 26 October 2024
Accepted: 26 October 2024
Published: 31 October 2024

Copyright: © 2024 by the authors. Licensee MDPI, Basel, Switzerland. This article is an open access article distributed under the terms and conditions of the Creative Commons Attribution (CC BY) license (https://creativecommons.org/licenses/by/4.0/).

1. Introduction

Global climate change is one of the most significant challenges facing the world today, with its widespread impact on Earth's ecosystems drawing considerable attention from the international community [1,2]. In arid regions, the effects of climate change are especially pronounced, as these vulnerable ecosystems are highly sensitive to climate fluctuations. Vegetation, a critical component of terrestrial ecosystems, is highly susceptible to variations in climate conditions [3,4]. The concepts of "Carbon Farming" and "Soil Carbon Sequestration" involve improving farming practices to increase the organic carbon

content in the soil, which helps mitigate climate change. [5]. Furthermore, forests in different regions play a significant role in absorbing atmospheric carbon dioxide. [6]. By analysing the effects of forest growth, forest management, and natural disturbances (such as wildfires and insect infestations) on the carbon sequestration capacity of forests, this study provides valuable insights into forest carbon dynamics. Therefore, studying vegetation dynamics in arid regions against the backdrop of climate change holds significant ecological and practical importance [7].

Vegetation in these regions is heavily dependent on water availability, with soil moisture (SM) being a key factor influencing vegetation growth [8,9]. SM serves as the link between the atmosphere, vegetation, soil, and groundwater, which reflects the Earth's water utilisation. SM significantly impacts vegetation growth and fractional vegetation cover (FVC) [10]. Under global climate change, variations in SM and vegetation growth are expected to significantly impact FVC. FVC is a key quantitative indicator for studying vegetation cover dynamics and effectively reflects vegetation trends and ecosystem health [11,12]. Amilcare Porporato and his team studied how vegetation cover in arid regions responds to changes in soil moisture, as well as the adaptation mechanisms of different vegetation types under drought stress [13]. Sonia Seneviratne's team investigated how global warming affects soil moisture and vegetation cover in arid regions [14]. By analysing climate models and observational data, they examined the impact of extreme climate events (such as heatwaves and prolonged droughts) on soil moisture and vegetation distribution in arid regions, particularly the constraints that water limitations impose on vegetation growth. Therefore, researching the spatiotemporal characteristics of SM and FVC in arid regions is essential for addressing global climate change, enhancing regional ecological protection, and promoting the sustainable development of natural resources.

In recent years, significant progress has been made in research on vegetation cover changes in arid regions. Particularly in Northwest China, many scholars have analysed the spatiotemporal changes in vegetation cover and its relationship with climate factors using remote sensing data and climate models [15]. These studies have shown that vegetation cover in China is highly sensitive to climate change, with variations in temperature (Tem) and precipitation (Pre) leading to significant changes in SM and FVC. However, existing studies are limited in terms of geographic coverage and data time scales. Longer time series of remote sensing data and higher spatial resolution are needed to better understand how different vegetation types respond to climate change across regions [16,17].

The methods used in this study are widely applied in vegetation change studies. The methods help to reveal long-term trends in vegetation cover in arid regions and their underlying climate drivers. In addition to the direct relationship between SM and FVC, global climate change also indirectly affects vegetation by altering regional hydrological cycles [18,19]. For example, changes in precipitation patterns and temperature owing to climate change alter evapotranspiration and water vapor exchange, which in turn affect SM and its ability to support vegetation growth. Studies have shown that, under the influence of climate change, the arid regions of Northwest China have experienced both warming and increased humidity. Water evaporation caused by rising temperatures and greater precipitation can promote vegetation growth, which enhances vegetation cover [20,21]. However, this process exhibits non-linear patterns, with warming and humidification demonstrating complex spatiotemporal variability.

The Heihe River basin serves as a prime example. As the second-largest inland river in Northwest China, the downstream areas of the Heihe River are characterised by a typical arid climate, with a highly fragile ecosystem [22]. The low vegetation cover of the region is particularly vulnerable to the impacts of climate change [23,24]. Therefore, studying the spatiotemporal characteristics of SM and FVC in the Heihe River basin and surrounding areas not only enhances our understanding of how climate change affects arid ecosystems but also provides scientific support for regional ecological protection and resource management [25,26]. In conclusion, this study aims to uncover the driving mechanisms behind vegetation cover changes in the context of climate change by analysing the spatiotempo-

ral characteristics of SM and FVC in the arid regions of Northwest China [27,28]. This research explores how different vegetation types respond to climate change by integrating remote sensing data with various analytical methods. The research provides scientific evidence to support ecosystem management and policy-making in the face of climate change challenges [29].

Water is a key factor influencing vegetation growth, community characteristics, and FVC in the lower reaches of the Heihe River, with climate change directly impacting its eco-hydrological processes [30,31]. Many researchers have studied groundwater, SM, salinity, and ecological water transmission to examine their effects on vegetation growth in this region, which has led to a range of valuable findings [32,33]. However, there is still a lack of sufficient research on climate change as a critical factor affecting the vegetation–soil–hydrological processes in the lower reaches of the Heihe River. In particular, the characteristics of FVC changes and their relationship to climate change remain unclear [34,35]. Furthermore, the natural vegetation in the lower reaches of the Heihe River serves as a primary barrier against wind and sand encroachment, which safeguards the ecosystem, and acts as a crucial ecological buffer zone that influences the ecological security of Northwest and North China [36–38]. This study investigates the spatiotemporal variations and responses of SM and vegetation cover in the arid zone of Northwest China in the context of climate change.

This study provides a detailed analysis of the relationship between vegetation cover changes in arid regions and global climate change. By elucidating how climate factors and soil moisture influence vegetation dynamics, it offers valuable insights into the complex interactions between climate and ecosystems. This paper specifically presents predictive insights into how climate change may impact ecosystems in arid regions, particularly in terms of changes in vegetation cover. These predictions are crucial for understanding potential future scenarios under various climate conditions. Based on the research findings, adaptive strategies for ecosystem management in response to climate change are proposed. These strategies, grounded in scientific evidence, aim to help policymakers, land managers, and local communities better adapt to the challenges posed by changing environmental conditions.

2. Materials and Methods

2.1. Study Area

The lower reaches of the Heihe River are located in Ejina Banner (39°52′–42°47′ N, 97°10′–103°7′ E) at the westernmost point of the Inner Mongolia Autonomous Region. Ejina Banner is bordered by Alxa Right Banner to the southeast, Gansu Province to the west and southwest, and Mongolia to the north. The elevation in this area ranges from 898 m to 1598 m and encompasses approximately 114,600 km^2 (Figure 1). Ejina Banner experiences a typical continental arid climate, characterised by dryness, low precipitation, high evaporation, abundant sunshine, and frequent sandstorms. The average annual temperature is 8.3 °C, while the average precipitation is 37.0 mm, and evaporation reaches 3841.5 mm. The region experiences frequent winds, often accompanied by sandstorms. The topography is predominantly characterised by Gobi, low mountains, deserts, rivers, lakes, and oases, with most of the area comprising Gobi deserts, which creates a transitional zone between oases and deserts. Vegetation is relatively sparse and primarily consists of desert riparian forests, desert shrublands, and desert meadows [39,40].

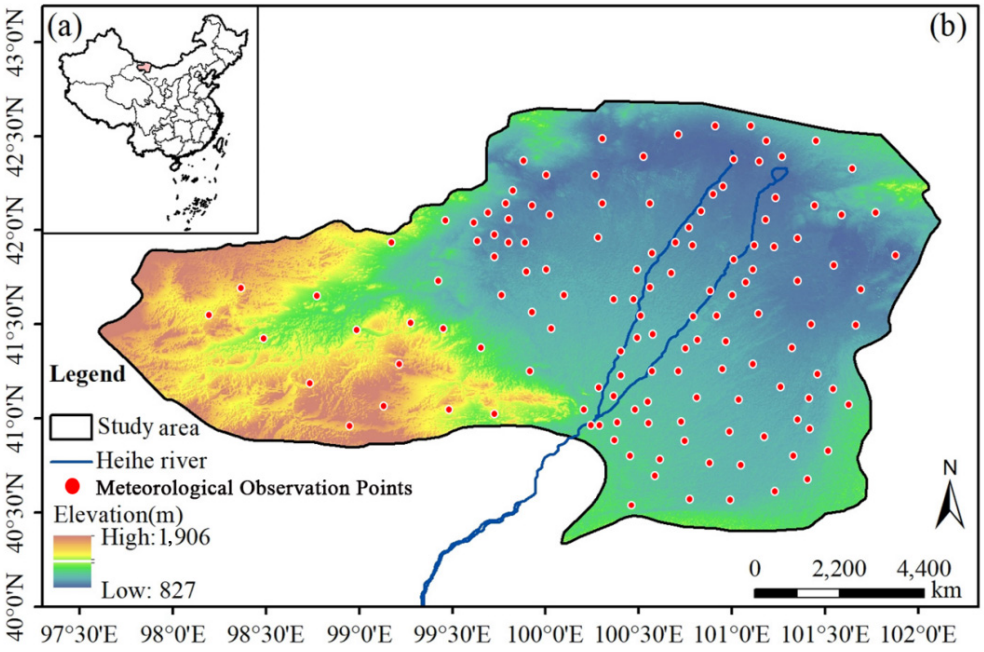


Figure 1. (**a**) Geographic location and boundaries of the Heihe River Basin and the study area. (**b**) Overview of the lower Heihe River topography.

2.2. Data Sources and Processing

The NDVI data used in this study were obtained from NASA (https://ladsweb.modaps.eosdis.nasa.gov/) (accessed on 19 September 2024). The data type is MOD13Q1 and covers the period from 2000 to 2022, with a spatial resolution of 250 m and a temporal resolution of 16 days. The maximum value composite method was applied to process the data, resulting in a 23-year interannual sequence dataset (Table 1).

Table 1. Data sources and formats used in this study.

Data Type	Source	Calculation	Time Series	Resolution	Abbreviation
NDVI	https://ladsweb.modaps.eosdis.nasa.gov/ (accessed on 19 September 2024)	Maximum value composite	2000–2022	250 m	NDVI
The mean annual temperature	Peng, S. (2020). 1 km monthly maximum temperature dataset for China (1901–2023). National Tibetan Plateau/Third Pole Environment Data Center. https://doi.org/10.5281/zenodo.3185722 (accessed on 19 September 2024)	Monthly data average	1901–2022	1 km	Tem
The mean annual precipitation	Peng, S. (2020). 1 km monthly precipitation dataset for China (1901–2023). National Tibetan Plateau/Third Pole Environment Data Center. https://doi.org/10.5281/zenodo.3114194 (accessed on 19 September 2024)	Monthly data summing	1901–2022	1 km	Pre
Soil moisture	https://data.tpdc.ac.cn (accessed on 19 September 2024)	Monthly data average	2000–2020	1 km	SM

Meteorological data, including Tem and Pre, were obtained from the China National Tibetan Plateau Data Center (http://data.tpdc.ac.cn) (accessed on 19 September 2024) covering the period from 1901 to 2022. The Pre data features a monthly dataset with

a resolution of 1 km for China, while the Tem data consists of a monthly maximum temperature dataset with the same resolution. The meteorological data were converted to Tif format, with monthly Pre data summed to derive annual precipitation and monthly Tem data averaged to calculate annual average temperature. Projection, resampling, and clipping operations were performed in ArcGIS to align the annual average temperature and annual average precipitation with the NDVI dataset in terms of pixel size and projection (Table 1).

The SM data used in this study were derived from satellite inversion of the global daily surface SM dataset, which has a resolution of 1 km and was released by the National Tibetan Plateau Science Data Centre (https://data.tpdc.ac.cn/) (accessed on 19 September 2024). This dataset provides monthly data spanning from 1 February 2000 to 31 December 2020.

Using the lower reaches of the Heihe River as a case study, the research utilises MOD13Q1-NDVI (Normalised Difference Vegetation Index) data from 2000 to 2022, along with Tem, Pre, and SM data from the same period. These data are employed to map the spatiotemporal dynamics of vegetation cover, assess its evolutionary trends, and explore the relationship between vegetation growth and Tem, Pre, and SM.

2.3. Research Methods

2.3.1. Calculation of Vegetation Cover

FVC exhibits a strong linear correlation with NDVI [41]. The integration of vegetation indices with the pixel dichotomy model effectively mitigates the impact of atmospheric and soil background factors and is widely used for estimating vegetation cover at both regional and global scales (Figure 2). Therefore, this study employed the pixel dichotomy model based on NDVI to estimate vegetation cover. The calculation of FVC is provided in Equation (1) [42,43].

$$FVC = \frac{NDVI - NDVI_{soil}}{NDVI_{veg} - NDVI_{soil}} \quad (1)$$

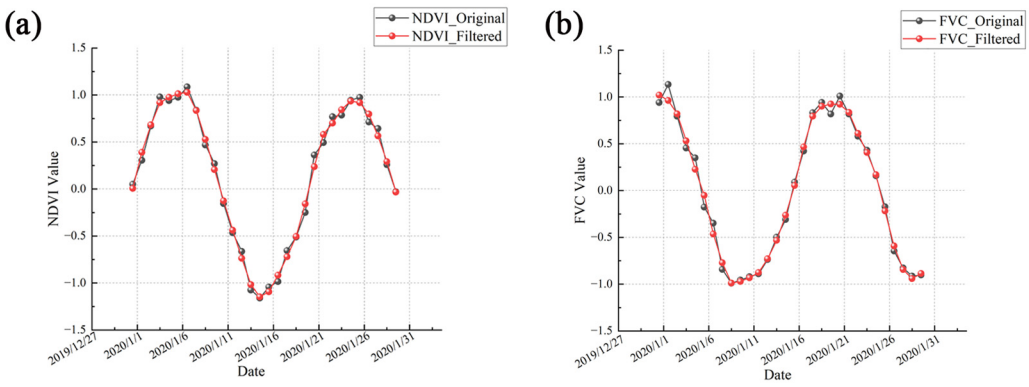


Figure 2. (**a**) The trend of the NDVI time series before and after applying the S-G filter. (**b**) The trend of the FVC time series before and after applying the S-G filter.

FVC represents the fractional vegetation cover, while NDVI refers to the normalised difference vegetation index for a unit grid. One of the variables denotes the NDVI value for bare soil or non-vegetated areas, which is theoretically close to 0, and indicates the NDVI value for fully vegetated areas, which is theoretically close to 1. Owing to the comprehensive influence of lighting conditions, image quality, vegetation types, and other factors, the actual values may vary. Values within the confidence interval of [5%, 95%] were selected as the values for the year. This study references the relevant literature on vegetation cover classification in arid regions [44,45]. According to field survey data, vegetation cover is classified into four levels: $0 \leq FVC < 0.05$ for no vegetation cover; $0.05 \leq FVC < 0.25$ for low vegetation cover; $0.25 \leq FVC < 0.50$ for medium vegetation cover; $0.50 \leq FVC < 1.00$ for high vegetation cover.

2.3.2. Stability Analysis

The coefficient of variation (C_v) quantifies the degree of data dispersion and is commonly used to represent the variability of a data series over a given study period. We can reveal the stability distribution characteristics of vegetation growth in the lower reaches of the Heihe River by calculating the pixel-by-pixel coefficient variation of vegetation cover data during the study period. The calculation of is provided in Equation (2) [46].

$$C_v = \frac{\sqrt{\frac{1}{n}\sum_{i=1}^{n}\left(FVC_i - \overline{FVC}\right)^2}}{\overline{FVC}} \quad (2)$$

where one of the variables is the vegetation cover value in the i-th year, another variable is the annual average vegetation cover during the study period, and n is the number of monitoring years.

2.3.3. Trend Analysis

Methodologically, the Mann–Kendall trend analysis, Theil–Sen slope estimator, and Hurst exponent are classical tools for studying the spatiotemporal trends of climate change and vegetation dynamics. The Mann–Kendall trend analysis is a non-parametric test commonly used to detect trends in time series data, while the Theil–Sen slope estimator assesses trend intensity by calculating the median slope between two points in a time series. The Hurst exponent is used to quantify long-term memory and autocorrelation in time series.

This study utilised the Theil–Sen trend analysis, the Mann–Kendall test, and the Hurst index to investigate the spatiotemporal changes, evolutionary trends, and sustainability characteristics of vegetation cover.

(1) Theil–Sen Trend Analysis and Mann–Kendall Test

Theil–Sen trend analysis and the Mann–Kendall test are non-parametric statistical methods that effectively mitigate issues related to data distribution and missing values. These methods are also resistant to the influence of outliers, leading to more robust and reliable results. The trend of vegetation cover change is defined by Equation (3) [47].

$$S_{FVC} = Median\left(\frac{FVC_j - FVC_i}{j - i}\right), 2000 \le i < j \le 2022 \quad (3)$$

When >0, it indicates an increasing trend in FVC, while <0 indicates a decreasing trend.

The Mann–Kendall test is used to assess the significance of trends [48]. The calculation formula is as follows:

For a set {} [36,49], I = 2000, 2001, . . ., 2022, the Z statistic is defined as follows:

$$Z = \begin{cases} \frac{S-1}{\sqrt{Var(S)}} & (S > 0) \\ 0 & (S = 0) \\ \frac{S+1}{\sqrt{Var(S)}} & (S < 0) \end{cases} \quad \text{Where } S = \sum_{i=1}^{n-1}\sum_{j=i+1}^{n} sign(x_j - x_i) \quad (4)$$

$$Sign(x_j - x_i) = \begin{cases} 1 & x_j - x_i \\ 0 & x_j - x_i \\ -1 & x_j - x_i \end{cases} \quad (5)$$

$$Var = \frac{n(n-1)(2n+5)}{18} \quad (6)$$

where two of the variables represent the FVC values in years j and i, respectively, and n is the length of the time series. The value range of Z is $(-\infty, +\infty)$. At a given significance level α, when $|Z| > u_{1-\alpha/2}$, it indicates a significant change in the study series at the α level [50,51].

(2) Hurst Index

The Hurst index is a useful method for quantitatively describing the dependence in a time series and is widely applied in studying vegetation cover changes to predict the developmental trends of FVC. The calculation steps are as follows [52]:

$$\overline{\xi_\tau} = \frac{1}{\tau}\sum_{\tau=1}^{\tau}\xi(t) \quad 1 \le t \le \tau = 1,2,3\ldots,n \tag{7}$$

$$X(t,\tau) = \sum_{n=1}^{t}\left(\xi(n) - \overline{\xi_\tau}\right) \tag{8}$$

$$R(\tau) = \max_{1\le t\le\tau} X(t,\tau) - \min_{1\le t\le\tau} X(t,\tau) \tag{9}$$

$$S(\tau) = \left[\frac{1}{\tau}\sum_{t=1}^{\tau}\left(\xi(t) - \overline{\xi_\tau}\right)^2\right]^{\frac{1}{2}} \tag{10}$$

$$\frac{R(\tau)}{S(\tau)} = (c\tau)^H \tag{11}$$

If the ratio follows the relation $R_{(\tau)}/S_{(\tau)} \triangleq R/S \propto \tau^H$, the time series exhibits the Hurst phenomenon, with H being the Hurst index. The value of H can take three forms: If $0 < H < 0.5$, it indicates anti-persistence in the FVC. If $H = 0.5$, it suggests that the FVC follows a random sequence. If $0.5 < H < 1$, it indicates persistence in the FVC.

3. Results

3.1. Spatiotemporal Distribution Characteristics

The spatial distribution of vegetation cover in the lower reaches of the Heihe River (Figure 3) shows that overall vegetation cover is relatively low, with areas of low vegetation cover being predominant. These low vegetation cover zones make up approximately 93.37% of the study area and are mainly concentrated in the Gobi desert region. Medium and high vegetation cover areas were smaller and covered 4.18% and 1.71% of the study area, respectively, and were mainly concentrated around the Ejina Oasis and Gurinai Lake. Figure 3 shows vegetation cover in the upper and lower sections of the East and West Rivers and the East and West Juyan Lakes regions. In contrast, the middle section of the East River and other Gobi regions display poorer vegetation cover. Thus, Ejina Banner, located in the westernmost part of Inner Mongolia, is predominantly desert and semi-desert. Vegetation growth largely depends on water replenishment from the middle and upper reaches of the Heihe River, which makes the ecological environment extremely fragile and highly vulnerable to climate change.

Between 2000 and 2022, the vegetation coverage in the lower reaches of the Heihe River showed a slow upward trend with fluctuations (Figure 3). The annual mean FVC value fluctuated within the range of 0.095 to 0.122, indicating relatively small fluctuations. However, the interannual variation trends in the areas of different vegetation coverage levels varied. The areas of medium and high vegetation coverage zones both showed an increasing trend, with increase rates of 37.14 km^2/a and 24.19 km^2/a, respectively (Figure 3e). In contrast, the areas of no coverage and low vegetation coverage zones showed a decreasing trend, with reduction rates of 54.87 km^2/a and 6.45 km^2/a, respectively. This indicates that areas of no vegetation and low vegetation coverage are transitioning towards zones with medium and high vegetation coverage.

Furthermore, through transition matrix analysis of FVC from 2020 to 2022, it was found that the areas of medium and high coverage increased the most, with increases of 854.19 km^2 and 556.37 km^2, respectively. The increase in medium coverage was mainly contributed to by the transition from low coverage, while the increase in high coverage was primarily due to the transition from medium coverage (Figure 3d). Overall, since the

implementation of ecological water delivery in the Heihe River in 2000, the vegetation in Ejina has shown significant improvement and recovery, which is consistent with related studies [40].

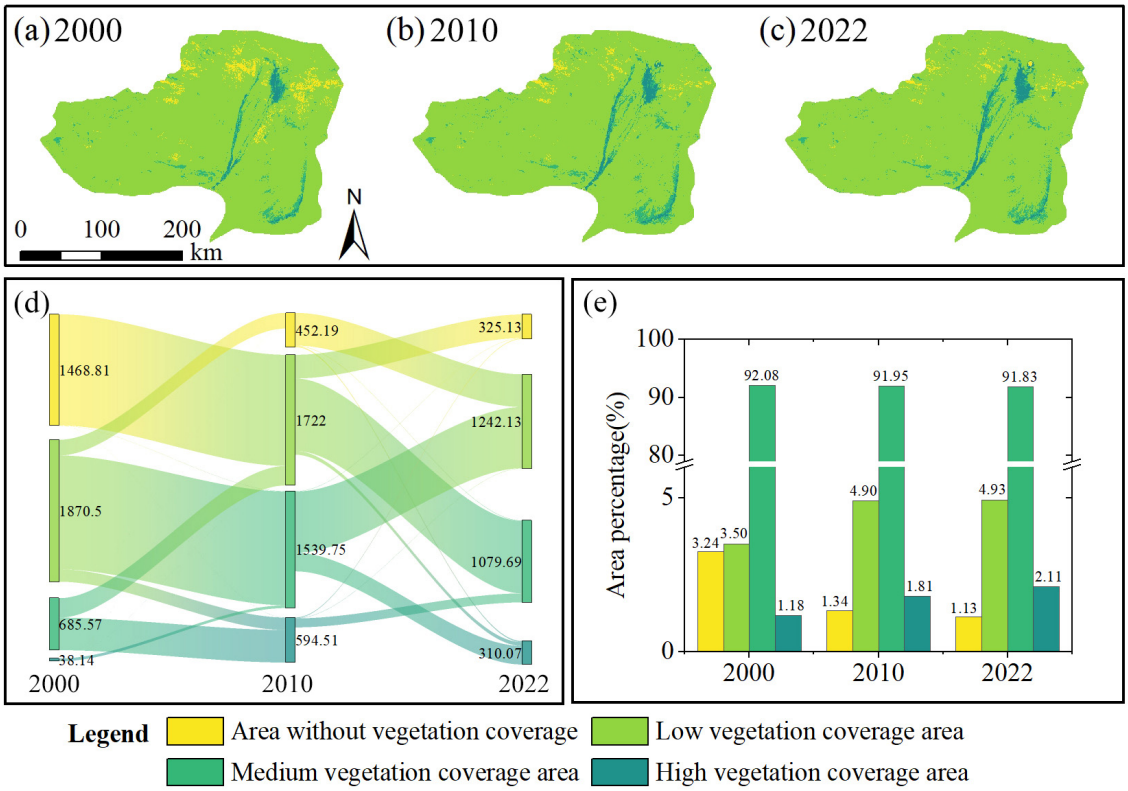


Figure 3. (**a**) Spatial distribution map of fractional vegetation cover in 2000, (**b**) spatial distribution map of fractional vegetation cover in 2010, (**c**) spatial distribution map of fractional vegetation cover in 2020, (**d**) vegetation cover class area transition diagram from 2000 to 2022, and (**e**) proportion of area for each vegetation cover class.

3.2. Stability Evaluation of Vegetation Cover Changes

The coefficient of variation (CV) was used as an indicator to evaluate vegetation stability, and the variation index was divided into five levels using the quantile method: high ($0 < CV \leq 0.11$), relatively high ($0.11 < CV \leq 0.16$), medium ($0.16 < CV \leq 0.21$), relatively low ($0.21 < CV \leq 0.31$), and low ($0.31 < CV \leq 2.83$). ArcGIS was used to calculate the area of each stability level. The majority of the study area's vegetation coverage fell within the relatively high or medium stability categories, accounting for 30.09% and 43.17% of the region, respectively. These areas were mostly located in desert regions with low vegetation coverage, consistent with the trend of minimal changes in the area of low vegetation coverage. Regions with relatively low and low stability accounted for 15.00% and 8.71% of the area, respectively, mainly distributed in the northern part of the lower reaches of the Heihe River, the lower reaches of the Donghe River, and the areas around East and West Juyan Lake (Figure 4a). This shows that the vegetation's ecological stability in the core oasis area of the lower reaches of the Heihe River is weak and highly susceptible to climate change and human activities, indicating high ecological vulnerability. Overall, the lower reaches of the Heihe River basin contain a large number of areas with low vegetation stability, particularly in the light green and dark green regions, indicating high ecological vulnerability in these areas. They are more susceptible to the impacts of climate change and human activities.

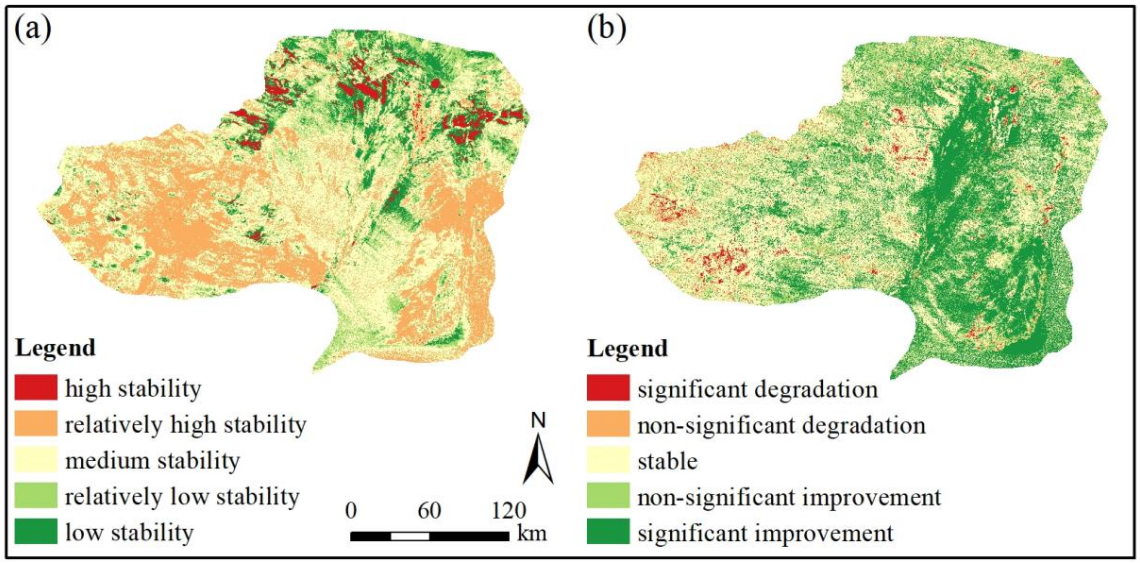


Figure 4. (**a**) Spatial distribution map illustrating the stability of land from the analyzed period, with varying levels of stability indicated by different colors: high stability, relatively high stability, medium stability, relatively low stability, and low stability. (**b**) Spatial distribution map indicating changes in land conditions, with categories such as significant degradation, non-significant degradation, stable areas, non-significant improvement, and significant improvement over time.

3.3. Dynamic Evolution Trends of Vegetation Cover

The Theil–Sen median trend analysis and Mann–Kendall test were employed to create a spatial distribution map of vegetation cover change trends in the lower reaches of the Heihe River (Figure 4b). The analysis revealed that vegetation improvement occurred over an area of 31,865.81 km^2 and accounted for 53.34% of the region, with significantly improved areas covering 19,112.38 km^2 (31.99%), mainly concentrated around the Ejina Oasis and Gurinai Lake. In contrast, the area of vegetation degradation was much smaller. It covered only 4180.50 km^2 in area, or 7% of the region. Therefore, over the past 23 years, the overall trend of vegetation cover in the lower reaches of the Heihe River has been one of improvement.

Overall, most areas of the Heihe River Basin exhibit low to medium Hurst index values (orange, yellow, and light green), indicating poor vegetation cover stability in these regions, especially in certain parts of the lower reaches of the Heihe River where the long-term trends of vegetation change are relatively uncertain. In contrast, the relatively high Hurst index in green areas reflects the relative stability of vegetation in a small portion of the Heihe River Basin. (Figure 5a). This suggests that the region overall displays weak anti-persistence, which indicates that future changes may reverse past trends. Coupling the linear fit slope with the Hurst index (Figure 5b) reveals that 4.81% of the area experienced continuous degradation, while 55.65% showed non-persistent improvement. Therefore, this study predicts that, without effective ecological protection measures, more than half of the vegetation in the lower reaches of the Heihe River is at risk of continuous degradation in the future.

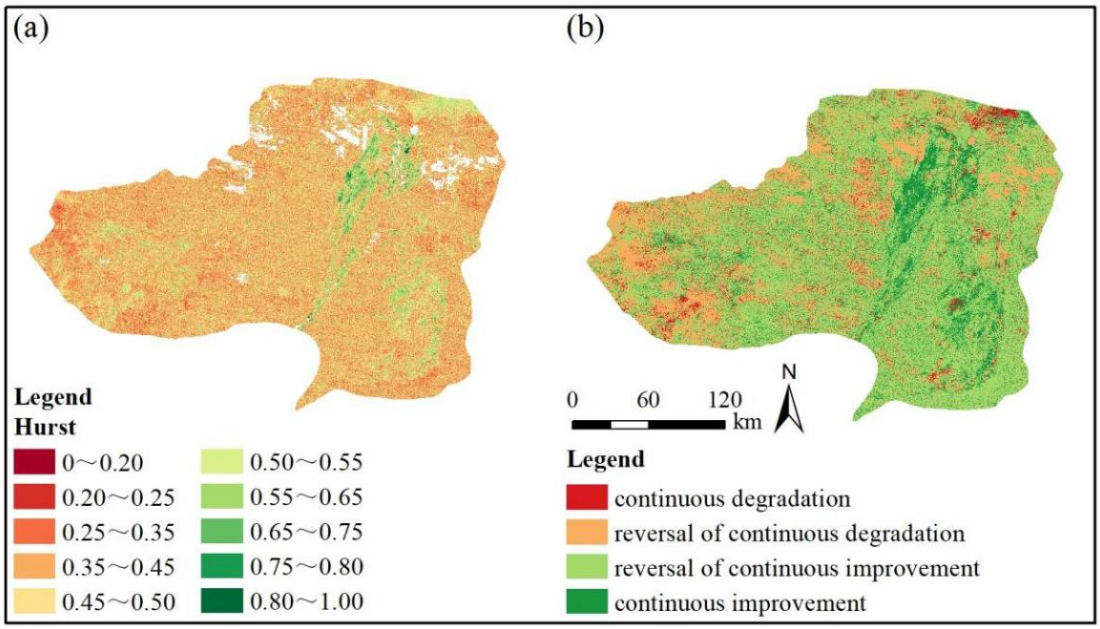


Figure 5. Hurst index (**a**) and future trend (**b**) of vegetation cover in the lower reaches of the Heihe River.

3.4. Response of Vegetation Cover to Climate Change

Existing studies have shown that climate change significantly affects vegetation cover in arid regions, with Tem and Pre being the most direct and sensitive climatic factors [44,53]. To examine how vegetation cover in the lower reaches of the Heihe River responds to climate change, this study analyses the correlation and impact trends using monthly Tem and Pre data from 2000 to 2022. As illustrated in Figure 6a, Tem exhibits a notable upward trend over the past 23 years, at a rate of 0.418 °C per decade, which is significant at the 0.05 level. This indicates a noticeable warming trend in the Ejina region, consistent with the warming patterns observed in Northwestern China. The annual Pre trend rate is −1.195 mm per decade, which signifies a slight but decreasing trend, accompanied by significant fluctuations in the curve. This suggests that precipitation in Ejina exhibits unstable interannual variability. Over the past 23 years, the Ejina region has experienced a gradual 'warming and drying' trend [54].

Pearson correlation analysis was applied to calculate the relationships among FVC, Tem, and Pre. The correlation coefficients between FVC and Tem in the study area range from 0.84 to −0.79 (Figure 6b). Regions with a significant positive correlation account for 9.98% of the area, mainly located in the southeastern part of the study area and along the Ejina River, where warming promotes vegetation growth. Conversely, regions with a significant negative correlation make up 1.06% of the area, scattered and discontinuously distributed, which indicates a threshold effect of Tem on vegetation growth, where further increases in Tem exacerbate drought and inhibit vegetation growth. The largest proportion of regions, approximately 88.96%, exhibit a non-significant correlation.

Compared with Tem, FVC exhibits a weaker correlation with Pre, with correlation coefficients ranging from 0.85 to −0.78 (Figure 6c). Regions with significant positive ($p < 0.01$), significant negative ($p < 0.05$), and non-significant correlations ($p > 0.05$) account for 6.94%, 0.98%, and 92.08% of the area, respectively. The areas with a positive correlation are mainly located in the southern part of the region, where the dry climate and herbaceous plant types make vegetation more sensitive to changes in precipitation, which enhances growth with increased Pre. Significant negative correlation areas are sporadically distributed in the central part of the study area and tend to decrease in size.

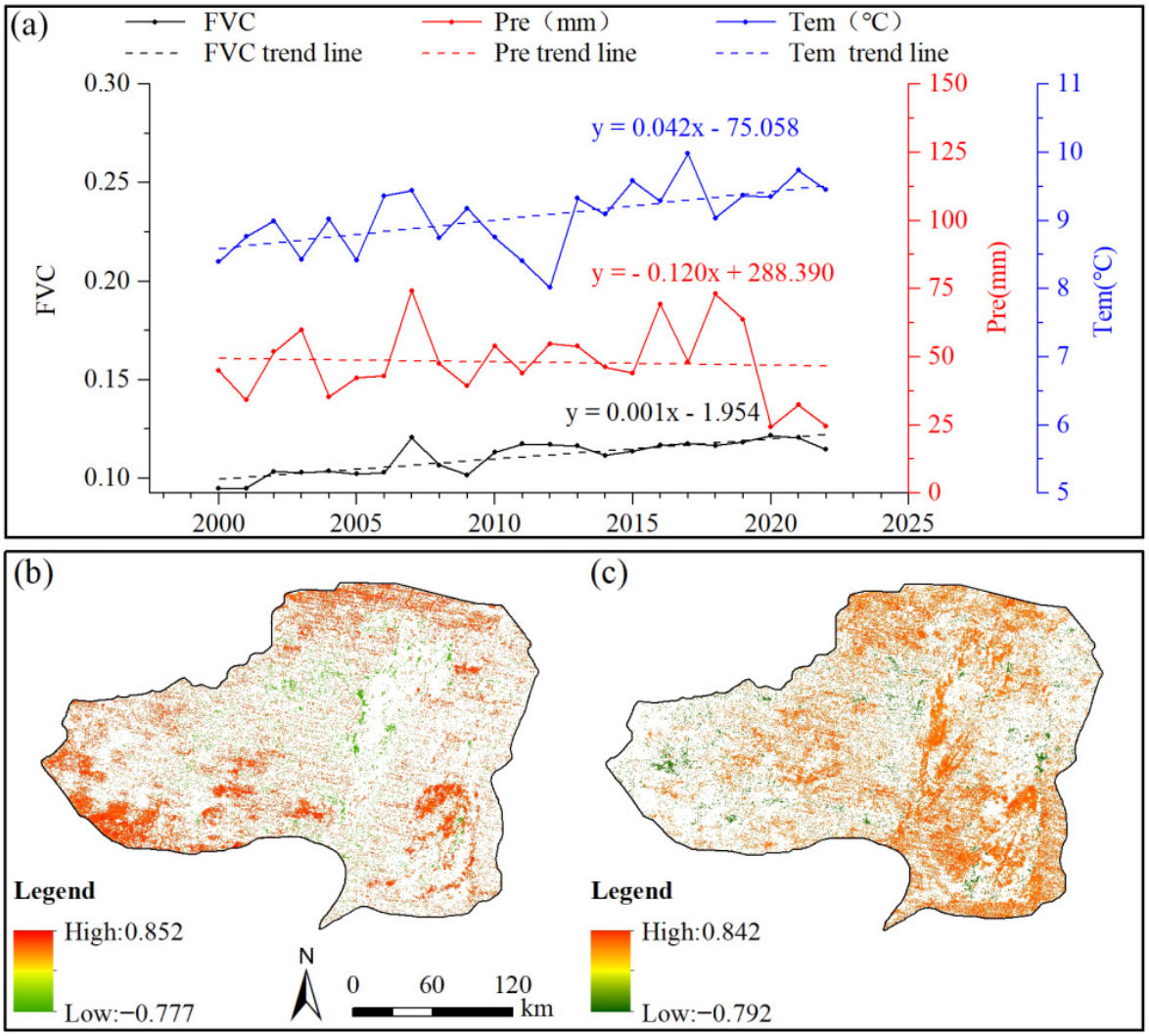


Figure 6. Trends of FVC, Pre, and Tem (**a**), the spatial distribution of correlation coefficients between FVC and Tem (**b**), and FVC and Pre (**c**).

The lower reaches of the Heihe River are situated in an arid to extremely arid climate region, where the average annual Pre is only 48.03 mm, and evaporation far exceeds Pre. Consequently, vegetation growth in these extremely water-scarce areas is highly dependent on the limited Pre, leading to a positive correlation between FVC and Pre. However, this correlation can be easily disrupted by natural and human factors, such as intensive agricultural irrigation near the Ejina River, which may weaken the relationship between climatic factors and FVC. In addition to Tem and Pre, vegetation cover in the lower reaches of the Heihe River is influenced by factors such as surface water, groundwater, and soil water–salt content [36,39]. This indicates that the vegetation ecosystem in this region remains fragile and is highly susceptible to climate change and human activities.

3.5. Relationship Between SM and NDVI

To analyse the impact of Tem and Pre on the seasonal variation of SM, a seasonal spatial distribution map of SM was created (Figure 7). The results indicate that the seasonal dynamics of SM in the lower reaches of the Heihe River are pronounced, with the highest SM observed in autumn at 10%, and the lowest levels occurring in summer and winter at 9.71%. The seasonal dynamics of SM in this region are mainly influenced by factors such as Tem, rainfall, and vegetation. The relationship between climatic factors and changes in SM is illustrated in Figure 8b,c. Spring (March to May) is identified as a critical recovery period

for SM in the lower reaches of the Heihe River. As Tem gradually rises, winter snow and ice begin to melt, leading to increased rainfall and a replenishment of SM. As the demand for water by vegetation increases, SM is rapidly consumed. In spring, SM fluctuates owing to the combined influences of Tem, rainfall, and vegetation. Summer (June to August) serves as the primary replenishment period for SM. Although high temperatures accelerate SM evaporation and intensify plant transpiration, increased rainfall steadily replenishes SM, resulting in a gradual increase. In autumn (September to November), as Tem and rainfall decrease, SM enters a period of stable consumption and exhibits a slow declining trend. In winter (December to February of the following year), as Tem and Pre decrease, snow is preserved owing to the low temperatures, keeping SM relatively stable. Although changes in SM during winter are minimal, they play an important role in replenishing SM in the following spring. Snowmelt is a crucial source of SM during this season.

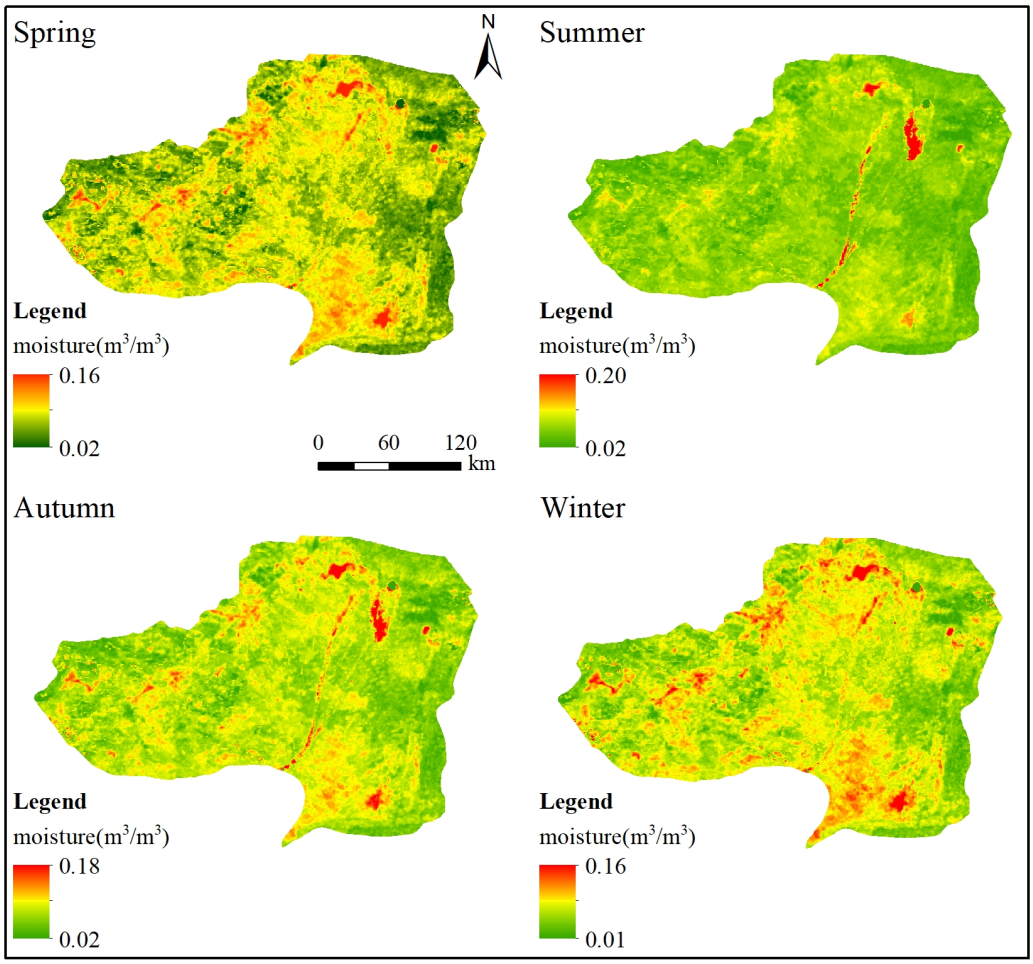


Figure 7. Seasonal spatial distribution of SM.

A correlation analysis was conducted between the NDVI during the growing season (May to September) and the corresponding SM. The correlation coefficients were classified into six levels: strong positive ($0.8 < R \leq 1$), moderate positive ($0.3 < R \leq 0.8$), weak positive ($0 < R \leq 0.3$), weak negative ($-0.3 \leq R < 0$), moderate negative ($-0.8 \leq R < -0.3$), and strong negative ($-1 \leq R < -0.8$). This analysis resulted in a distribution map illustrating the correlation between NDVI and SM in the lower reaches of the Heihe River (Figure 8a). The findings revealed that NDVI is weakly positively correlated with SM in most areas, particularly in regions with low vegetation cover, primarily in desert and Gobi areas, which account for approximately 66.1% of the study region. This suggests that in these remote desert areas, vegetation is significantly constrained by hydrological conditions,

such as surface water and groundwater, which makes it more susceptible to variations in SM and results in a positive correlation [55,56]. However, the correlation is relatively weak. Although an increase in SM can promote vegetation growth to some extent, it is also influenced by climatic conditions, soil texture, and soil salinity.

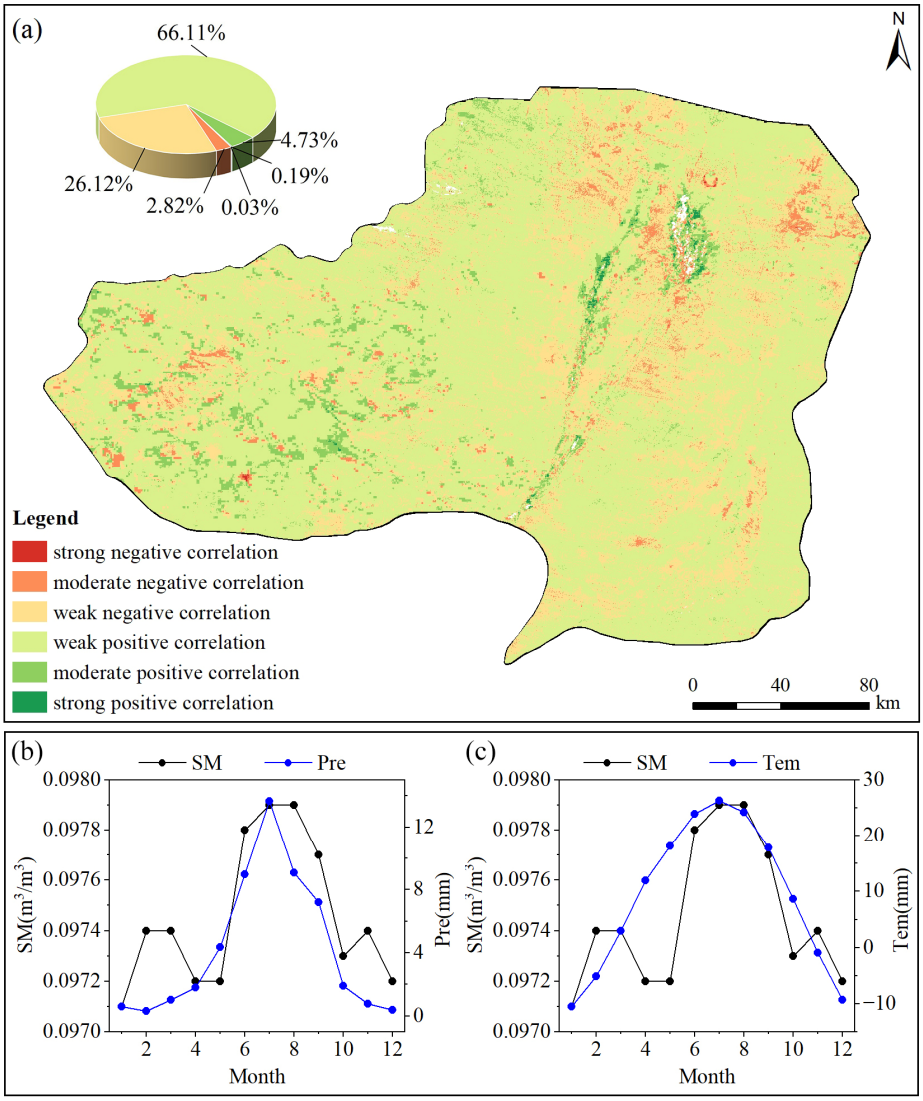


Figure 8. (**a**) Spatial distribution map showing the correlation between NDVI and SM during the vegetation growing season (May to September); (**b**) monthly variation trend of SM in relation to Pre; (**c**) monthly variation trend of SM in relation to Tem.

4. Discussion

4.1. Climate Change in the Lower Reaches of the Heihe River Under Global Climate Change

Global climate change is one of the most pressing challenges of our time, which profoundly affects climate systems worldwide. Arid regions, characterised by unique climatic conditions and environmental sensitivity, respond markedly to global climate change [57]. Global warming has generally resulted in rising temperatures in these areas, accelerated moisture evaporation, and exacerbated drought conditions. In recent decades, temperatures in arid regions have increased significantly at a rate of 0.032 °C per year, which reflects an accelerating warming and drying trend. The impact of global climate change on precipitation in arid regions is more complex, with varying effects across different areas [54]. Some areas may experience reduced precipitation, which exacerbates drought conditions, while others may see increased precipitation, which indicates a 'wetting' trend.

Additionally, climate change may result in more pronounced seasonal and spatial variations in precipitation, particularly in terms of timing and intensity. Some arid regions might experience more concentrated precipitation and more frequent extreme rainfall events, leading to flooding, even as the overall climate becomes drier.

The lower reaches of the Heihe River, located in the high-latitude arid region of Northwest China, exhibit strong continental climate characteristics and are significantly affected by global climate change [58]. Since the 1980s, particularly after 1986, temperatures in this region have shown a marked warming trend, although the rate of increase varies by season. Winter temperatures have increased the most, while spring temperatures have increased the least, which is somewhat inconsistent with the broader climatic changes observed in Northwest China and Inner Mongolia [59]. Precipitation in the lower reaches of the Heihe River has shown significant decadal variability. The 1960s and 1990s recorded higher precipitation than the overall average, while other decades exhibited a decreasing trend. Since 2000, annual precipitation has alternated between positive and negative anomalies, with an overall declining trend, particularly after 2018, when precipitation consistently decreased. This indicates that, while global climate change impacts the lower reaches of the Heihe River, regional climate changes also exhibit local peculiarities. The significant temperature increase, high evaporation rates, and reduced precipitation of the region have led to a warmer, drier climate, which poses serious threats to vegetation growth.

4.2. Relationship Between Vegetation Dynamics and Climate Change in the Lower Reaches of the Heihe River

Arid regions, among the most vulnerable ecosystems on Earth, display complex interactions between vegetation dynamics and climate change. Rising temperatures can accelerate plant transpiration and increase water stress, while reduced precipitation limits SM replenishment. These changes may lead to reduced vegetation cover, ecosystem degradation, and an increased risk of desertification. The study results show a generally weak correlation between vegetation cover changes and Tem and Pre in the lower reaches of the Heihe River. However, a unique feedback mechanism has developed between regional vegetation and climate. In this extremely arid continental climate, the vegetation—comprising species such as *Populus euphratica*, *Haloxylon ammodendron*, *Elaeagnus angustifolia*, and desert shrubs such as Reaumuria soongorica and Calligonum mongolicum—has adapted to drought conditions [39]. With ongoing warming and intensified evaporation, SM dissipation accelerates, which increases the risk of surface vegetation survival. Some ecosystems in the region have shifted from functional to structural decline, as riparian forests gradually transform into shrub and semi-shrub desert landscapes, and hydrophytic herbaceous plants are replaced by xerophytic species. This underscores the significant impact of climate change on the vegetation ecosystems in the lower reaches of the Heihe River.

As a crucial component of the ecosystem, vegetation changes have feedback effects on regional climate. Research shows that vegetation cover changes can influence climate by regulating the surface energy balance, which alters surface albedo, and affects evapotranspiration [60]. When vegetation cover declines, surface albedo increases, which reduces the absorption of shortwave radiation and creates a cooling effect. However, vegetation degradation also exposes more surface area, intensifies evaporation, and exacerbates regional aridity. Vegetation changes further impact local and regional water cycles through transpiration, with reduced cover potentially lowering transpiration rates and altering precipitation patterns. Therefore, the feedback effect of vegetation cover changes on temperature is a complex process with disputed mechanisms [61]. Nonetheless, it is widely agreed that changes in vegetation cover and precipitation have a mutually reinforcing feedback effect.

5. Conclusions

This study examines the spatiotemporal characteristics of vegetation cover and its response to climate change in the lower reaches of the Heihe River, an arid region in

Northwest China. Using MOD13Q1-NDVI data from 2000 to 2022, along with Tem and Pre data for the same period, the main conclusions are as follows:

(1) The lower reaches of the Heihe River are predominantly characterised by low vegetation cover or areas lacking vegetation. Medium to high vegetation cover is mainly concentrated along riverbanks and in the Juyan Lake region and forms the Ejina River Oasis landscape. From 2000 to 2022, overall vegetation cover in the region exhibits a slow but fluctuating upward trend, with signs of degradation stabilising and showing improvement;

(2) The ecological stability of vegetation in the core oasis area of the lower reaches of the Heihe River is weak and highly susceptible to climate change and human activities. The vegetation ecosystem exhibits a high degree of vulnerability. In terms of evolutionary trends, vegetation cover has generally improved over the past 23 years. However, future changes are expected to show weak non-persistence, meaning that the region's vegetation still faces a significant risk of degradation;

(3) Climate change in the lower reaches of the Heihe River is influenced by global patterns but also exhibits local climatic peculiarities. The region has experienced a notable warming trend, consistent with global and Northwestern China trends, though the rate of warming varies seasonally. Precipitation has shown a slight decreasing trend with highly unstable decadal variations. Overall, the regional climate demonstrates a 'warming and drying' trend, which poses severe threats and challenges to vegetation growth;

(4) The changes in vegetation cover are generally weakly correlated with temperature and precipitation, although temperature has a slightly greater impact on vegetation cover changes. An increase in temperature to some extent promotes the growth of plants along the river, while it inhibits the growth of drought-tolerant desert plants. An increase in precipitation can also promote plant growth to a certain degree. However, the evaporation rate in the study area far exceeds the amount of precipitation, and factors such as surface water, groundwater, and soil salinity are more sensitive to plant growth. Therefore, the contribution of the area's minimal rainfall to plant growth is relatively weak.

Author Contributions: Conceptualisation, X.P., M.F., W.W. and H.Z.; Formal analysis, L.M., X.P., C.H. and D.S.; Methodology, L.M., X.P. and W.W.; Project administration, P.B., M.F., H.Z., W.Z. and G.T.; Software, L.M., X.P., C.H. and D.S.; Validation, L.M. and X.P.; Visualisation, X.P.; Writing—original draft, X.P.; Writing—review and editing, L.M. and X.P. All authors have read and agreed to the published version of the manuscript.

Funding: This research was funded by the Science and Technology Innovation Foundation of Command Center of Integrated Natural Resources Survey Center, grant number KC20220010; China Geological Survey project, grant number DD20242704 and DD20242037.

Data Availability Statement: Data will be made available on request.

Acknowledgments: This work was jointly supported by the Science and Technology Innovation Foundation of Command Center of Integrated Natural Resources Survey Center (KC20220010), the project from China Geological Survey [DD20242704] [DD20242037], and the project from Key Laboratory of Tropical Island Land Surface processes and Environmental Changes of Hainan Province (DLZDSYS202404), and the project from Key Lab. of Biodiversity Conservation and Characteristic Resource Utilization in Southwest Anhui (Wxn202428).

Conflicts of Interest: The authors declare no conflicts of interest.

References

1. Hoegh-Guldberg, O.; Jacob, D.; Taylor, M.; Guillén Bolaños, T.; Bindi, M.; Brown, S.; Camilloni, I.; Diedhiou, A.; Djalante, R.; Ebi, K. The human imperative of stabilizing global climate change at 1.5 °C. *Science* **2019**, *365*, eaaw6974. [CrossRef] [PubMed]
2. Häyhä, T.; Lucas, P.; van Vuuren, D.; Cornell, S.; Hoff, H. From Planetary Boundaries to national fair shares of the global safe operating space—How can the scales be bridged? *Glob. Environ. Change* **2016**, *40*, 60–72. [CrossRef]

3. Perry, L.; Andersen, D.; Reynolds, L.; Nelson, S.; Shafroth, P. Vulnerability of riparian ecosystems to elevated CO2 and climate change in arid and semiarid western North America. *Glob. Change Biol.* **2012**, *18*, 821–842. [CrossRef]
4. Antala, M.; Juszczak, R.; van der Tol, C.; Rastogi, A. Impact of climate change-induced alterations in peatland vegetation phenology and composition on carbon balance. *Sci. Total Environ.* **2022**, *827*, 154294. [CrossRef]
5. Lal, R. Soil carbon management and climate change. *Carbon Manag.* **2013**, *4*, 439–462. [CrossRef]
6. Pan, Y.; Birdsey, R.A.; Fang, J.; Houghton, R.; Kauppi, P.E.; Kurz, W.A.; Phillips, O.L.; Shvidenko, A.; Lewis, S.L.; Canadell, J.G. A large and persistent carbon sink in the world's forests. *Science* **2011**, *333*, 988–993. [CrossRef]
7. Jiang, H.; Xu, X.; Guan, M.; Wang, L.; Huang, Y.; Jiang, Y. Determining the contributions of climate change and human activities to vegetation dynamics in agro-pastural transitional zone of northern China from 2000 to 2015. *Sci. Total Environ.* **2020**, *718*, 134871. [CrossRef]
8. Deng, Y.; Wang, S.; Bai, X.; Luo, G.; Wu, L.; Chen, F.; Wang, J.; Li, C.; Yang, Y.; Hu, Z. Vegetation greening intensified soil drying in some semi-arid and arid areas of the world. *Agric. For. Meteorol.* **2020**, *292*, 108103. [CrossRef]
9. Li, W.; Migliavacca, M.; Forkel, M.; Denissen, J.; Reichstein, M.; Yang, H.; Duveiller, G.; Weber, U.; Orth, R. Widespread increasing vegetation sensitivity to soil moisture. *Nat. Commun.* **2022**, *13*, 3959. [CrossRef]
10. Anees, S.A.; Mehmood, K.; Rehman, A.; Rehman, N.U.; Muhammad, S.; Shahzad, F.; Hussain, K.; Luo, M.; Alarfaj, A.A.; Alharbi, S.A. Unveiling Fractional Vegetation Cover Dynamics: A Spatiotemporal Analysis Using MODIS NDVI and Machine Learning. *Environ. Sustain. Indic.* **2024**, *24*, 100485. [CrossRef]
11. Liu, H.; Li, X.; Mao, F.; Zhang, M.; Zhu, D.E.; He, S.; Huang, Z.; Du, H. Spatiotemporal evolution of fractional vegetation cover and its response to climate change based on MODIS data in the subtropical region of China. *Remote Sens.* **2021**, *13*, 913. [CrossRef]
12. Fu, B.; Yang, W.; Yao, H.; He, H.; Lan, G.; Gao, E.; Qin, J.; Fan, D.; Chen, Z. Evaluation of spatio-temporal variations of FVC and its relationship with climate change using GEE and Landsat images in Ganjiang River Basin. *Geocarto Int.* **2022**, *37*, 13658–13688. [CrossRef]
13. Porporato, A.; Laio, F.; Ridolfi, L.; Rodriguez-Iturbe, I. Plants in water-controlled ecosystems: Active role in hydrologic processes and response to water stress: III. Vegetation water stress. *Adv. Water Resour.* **2001**, *24*, 725–744. [CrossRef]
14. Seneviratne, S.I.; Zhang, X.; Adnan, M.; Badi, W.; Dereczynski, C.; Luca, A.D.; Ghosh, S.; Iskandar, I.; Kossin, J.; Lewis, S. *Weather and Climate Extreme Events in a Changing Climate*; Cambridge University Press: Cambridge, UK, 2021; pp. 1513–1766. [CrossRef]
15. Wang, F.; Pan, X.; Gerlein-Safdi, C.; Cao, X.; Wang, S.; Gu, L.; Wang, D.; Lu, Q. Vegetation restoration in Northern China: A contrasted picture. *Land Degrad. Dev.* **2020**, *31*, 669–676. [CrossRef]
16. Ma, M.; Wang, Q.; Liu, R.; Zhao, Y.; Zhang, D. Effects of climate change and human activities on vegetation coverage change in northern China considering extreme climate and time-lag and -accumulation effects. *Sci. Total Environ.* **2023**, *860*, 160527. [CrossRef] [PubMed]
17. Beamish, A.; Raynolds, M.K.; Epstein, H.; Frost, G.V.; Macander, M.J.; Bergstedt, H.; Bartsch, A.; Kruse, S.; Miles, V.; Tanis, C.M. Recent trends and remaining challenges for optical remote sensing of Arctic tundra vegetation: A review and outlook. *Remote Sens. Environ.* **2020**, *246*, 111872. [CrossRef]
18. Almalki, R.; Khaki, M.; Saco, P.M.; Rodriguez, J.F. Monitoring and mapping vegetation cover changes in arid and semi-arid areas using remote sensing technology: A review. *Remote Sens.* **2022**, *14*, 5143. [CrossRef]
19. Zhang, E.; Liu, Y.; Pan, T.; Tan, Q.; Ma, Z. Evaluating the effects of climate change and human activities on the seasonal trends and spatial heterogeneity of soil moisture. *Remote Sens.* **2022**, *14*, 4862. [CrossRef]
20. Yang, L.; Feng, Q.; Adamowski, J.F.; Alizadeh, M.R.; Yin, Z.; Wen, X.; Zhu, M. The role of climate change and vegetation greening on the variation of terrestrial evapotranspiration in northwest China's Qilian Mountains. *Sci. Total Environ.* **2021**, *759*, 143532. [CrossRef]
21. Zhang, Q.; Yang, J.; Wang, W.; Ma, P.; Lu, G.; Liu, X.; Yu, H.; Fang, F. Climatic warming and humidification in the arid region of Northwest China: Multi-scale characteristics and impacts on ecological vegetation. *J. Meteorol. Res.* **2021**, *35*, 113–127. [CrossRef]
22. Shao, Y.; Jiang, Q.O.; Wang, C.; Wang, M.; Xiao, L.; Qi, Y. Analysis of critical land degradation and development processes and their driving mechanism in the Heihe River Basin. *Sci. Total Environ.* **2020**, *716*, 137082. [CrossRef] [PubMed]
23. Maja, M.M.; Ayano, S.F. The impact of population growth on natural resources and farmers' capacity to adapt to climate change in low-income countries. *Earth Syst. Environ.* **2021**, *5*, 271–283. [CrossRef]
24. Halofsky, J.E.; Peterson, D.L.; Harvey, B.J. Changing wildfire, changing forests: The effects of climate change on fire regimes and vegetation in the Pacific Northwest, USA. *Fire Ecol.* **2020**, *16*, 4. [CrossRef]
25. Wang, Y.; Wang, J.; Zhang, Q. Analysis of ecological drought risk characteristics and leading factors in the Yellow River Basin. *Theor. Appl. Climatol.* **2024**, *155*, 1739–1757. [CrossRef]
26. Zhang, J.; Guan, Q.; Du, Q.; Ni, F.; Mi, J.; Luo, H.; Shao, W. Spatial and temporal dynamics of desertification and its driving mechanism in Hexi region. *Land Degrad. Dev.* **2022**, *33*, 3539–3556. [CrossRef]
27. Zhou, Q.; Wei, C.; Wang, H.; Wang, D. Spatiotemporal evolution and driving factors analysis of fractional vegetation coverage in the arid region of northwest China. *Sci. Total Environ.* **2024**, *954*, 176271. [CrossRef]
28. Han, H.; Yin, Y.; Zhao, Y.; Qin, F. Spatiotemporal Variations in Fractional Vegetation Cover and Their Responses to Climatic Changes on the Qinghai–Tibet Plateau. *Remote Sens.* **2023**, *15*, 2662. [CrossRef]
29. Xavier, L.Y.; Guilhon, M.; Gonçalves, L.R.; Corrêa, M.R.; Turra, A. Waves of change: Towards ecosystem-based management to climate change adaptation. *Sustainability* **2022**, *14*, 1317. [CrossRef]

30. Jiao, A.; Wang, Z.; Deng, X.; Ling, H.; Chen, F. Eco-Hydrological Response of Water Conveyance in the Mainstream of the Tarim River, China. *Water* **2022**, *14*, 2622. [CrossRef]
31. Yi, F.; Lu, Q.; Li, Y.; Wang, Z.; Yao, B.; Yang, Q.; Wang, J. Ecological vulnerability assessment of natural oasis in arid areas: Application to Dunhuang, China. *Ecol. Indic.* **2023**, *149*, 110139. [CrossRef]
32. Ding, J.; Zhao, W.; Daryanto, S.; Wang, L.; Fan, H.; Feng, Q.; Wang, Y. The spatial distribution and temporal variation of desert riparian forests and their influencing factors in the downstream Heihe River basin, China. *Hydrol. Earth Syst. Sci.* **2017**, *21*, 2405–2419. [CrossRef]
33. Song, X.; Liao, J.; Xue, X.; Ran, Y. Multi-sensor evaluating effects of an ecological water diversion project on land degradation in the Heihe River Basin, China. *Front. Environ. Sci.* **2020**, *8*, 152. [CrossRef]
34. Zhang, M.; Wang, S.; Fu, B.; Gao, G.; Shen, Q. Ecological effects and potential risks of the water diversion project in the Heihe River Basin. *Sci. Total Environ.* **2018**, *619*, 794–803. [CrossRef]
35. Zhao, Y.; Wei, Y.; Li, S.; Wu, B. Downstream ecosystem responses to middle reach regulation of river discharge in the Heihe River Basin, China. *Hydrol. Earth Syst. Sci.* **2016**, *20*, 4469–4481. [CrossRef]
36. Dong, G.; Lian, Y.; Fan, Z.; Chang, X.; Gu, J. Vegetation Changes of Ejina Oasis in the Lower Reaches of Heihe River Before and After Ecological Scheduling for Water Resources. *Yellow River* **2019**, *41*, 5–9. [CrossRef]
37. Da, L.; Ma, J. Current ecological status and its trend of the Ejin River of the downstream Heihe River. *Environ. Dev.* **2014**, *26*, 171–174. [CrossRef]
38. Nian, Y.; Wang, X.; Cai, D. Analysis on Climate and Ecological Environment Change in the Ejin Delta, the Lower Reaches of the Heihe River. *J. Arid Meteorol.* **2015**, *33*, 28–37. [CrossRef]
39. Si, R.; Liu, B.; Zhao, W.; Zhu, Z.; Zhao, Y. Species diversity and stability patterns of plant communities in the tail area of the Heihe River. *J. Desert Res.* **2021**, *41*, 174–184. [CrossRef]
40. Wang, C.; Zhang, Y.; Zhao, W. Eco-hydrological restoration effect of ecological water conveyance in Ejina oasis, lower reaches of the Heihe River in recent 20 years. *Chin. J. Ecol.* **2022**, *41*, 2180–2187. [CrossRef]
41. Gutman, G.; Ignatov, A. The derivation of the green vegetation fraction from NOAA/AVHRR data for use in numerical weather prediction models. *Int. J. Remote Sens.* **1998**, *19*, 1533–1543. [CrossRef]
42. Huo, H.; Sun, C. Spatiotemporal variation and influencing factors of vegetation dynamics based on Geodetector: A case study of the northwestern Yunnan Plateau, China. *Ecol. Indic.* **2021**, *130*, 108005. [CrossRef]
43. Mingtan, S.; Tan, B.; Hou, R.; Huang, Y. A dataset of spatial-temporal changes of vegetation coverage with a spatial resolution of 30m in the Pearl River Delta from 2000 to 2020. *China Sci. Data* **2023**, *8*, 471–483. [CrossRef]
44. Zheng, Y.; Zhang, L.; Zhou, Y.; Zhang, B. Vegetation Change and Its Driving Factors in Global Drylands during the Period of 1982–2012. *Arid Zone Res.* **2017**, *34*, 59–66. [CrossRef]
45. You, Q.; Xu, B.; Zou, S.; Qin, Y.; Wang, D.; Yu, D. The vegetation-climate quantitative relationship and characteristics in arid and semi-arid region of northern China. *J. Desert Res.* **2023**, *43*, 274–287. [CrossRef]
46. Castagliola, P.; Celano, G.; Psarakis, S. Monitoring the coefficient of variation using EWMA charts. *J. Qual. Technol.* **2011**, *43*, 249–265. [CrossRef]
47. Yue, S.; Pilon, P.; Cavadias, G. Power of the Mann–Kendall and Spearman's rho tests for detecting monotonic trends in hydrological series. *J. Hydrol.* **2002**, *259*, 254–271. [CrossRef]
48. Yuan, L.; Jiang, W.; Shen, W.; Liu, Y.; Wang, W.; Tao, L.; Zheng, H.; Liu, X. Spatial and temporal changes of vegetation cover in the Yellow River Basin from 2000 to 2010. *Acta Ecol. Sin.* **2013**, *33*, 7798–7806. [CrossRef]
49. Sutton, A.; Fisher, A.; Metternicht, G. Assessing the accuracy of Landsat vegetation fractional cover for monitoring Australian drylands. *Remote Sens.* **2022**, *14*, 6322. [CrossRef]
50. Wang, J.; Xie, Y.; Wang, X.; Dong, J.; Bie, Q. Detecting Patterns of Vegetation Gradual Changes (2001–2017) in Shiyang River Basin, Based on a Novel Framework. *Remote Sens.* **2019**, *11*, 2475. [CrossRef]
51. Ghorbanian, A.; Mohammadzadeh, A.; Jamali, S. Linear and Non-Linear Vegetation Trend Analysis throughout Iran Using Two Decades of MODIS NDVI Imagery. *Remote Sens.* **2022**, *14*, 3683. [CrossRef]
52. Kang, Y.; Guo, E.; Wang, Y.; Bao, Y.; Bao, Y.; Na, R. Application of temperature vegetation dryness index for drought monitoring in Mongolian Plateau. *J. Appl. Ecol.* **2021**, *32*, 2534–2544. [CrossRef]
53. Jiang, W.; Niu, Z.; Wang, L.; Yao, R.; Gui, X.; Xiang, F.; Ji, Y. Impacts of drought and climatic factors on vegetation dynamics in the Yellow River Basin and Yangtze River Basin, China. *Remote Sens.* **2022**, *14*, 930. [CrossRef]
54. Ding, Y.; Liu, Y.; Xu, Y.; Wu, P.; Xue, T.; Wang, J.; Shi, Y.; Zhang, Y.; Song, Y.; Wang, P. Regional Responses to Global Climate Change: Progress and Prospects for Trend, Causes, and Projection of Climatic Warming-Wetting in Northwest China. *Adv. Earth Sci.* **2023**, *38*, 551–562. [CrossRef]
55. Shi, X.; Ishtiaq, U.; Din, M.; Akram, M. Fractals of Interpolative Kannan Mappings. *Fractal Fract.* **2024**, *8*, 493. [CrossRef]
56. Han, G.; Xu, J.; Zhang, X.; Pan, X. Efficiency and Driving Factors of Agricultural Carbon Emissions: A Study in Chinese State Farms. *Agriculture* **2024**, *14*, 1454. [CrossRef]
57. Hegerl, G.C.; Taylor, K.L. Last year's summer was the warmest in 2000 years. *Nature* **2024**, *631*, 35–36. [CrossRef]
58. Liu, Q.; Cheng, P.; Lyu, M.; Yan, X.; Xiao, Q.; Li, X.; Wang, L.; Bao, L. Impacts of Climate Change on Runoff in the Heihe River Basin, China. *Atmosphere* **2024**, *15*, 516. [CrossRef]

59. Zhang, H.; Han, F.; Zhang, L.; Wang, L.; Sun, Y.; Li, F. Analysis of spatial and seasonal variations in climate warming and humidification in Northwest China. *Arid Zone Res.* **2023**, *40*, 517–531. [CrossRef]
60. Li, H.; Zhang, Y.; Vaze, J.; Wang, B. Separating effects of vegetation change and climate variability using hydrological modelling and sensitivity-based approaches. *J. Hydrol.* **2011**, *420*, 403–418. [CrossRef]
61. Zhao, D.; Wang, K.; Cui, Y. Feedback mechanisms and regulatory effects of vegetation change on climate. *Acta Ecol. Sin.* **2023**, *43*, 7830–7840. [CrossRef]

Disclaimer/Publisher's Note: The statements, opinions and data contained in all publications are solely those of the individual author(s) and contributor(s) and not of MDPI and/or the editor(s). MDPI and/or the editor(s) disclaim responsibility for any injury to people or property resulting from any ideas, methods, instructions or products referred to in the content.